

A Fast Iterative Shrinkage-Thresholding Algorithm for Electrical Resistance Tomography

Zhang lingling
Department of Mathematics, Tianjin
University
Tianjin, China
zhanglingling@tju.edu.cn

Wang huaxiang, Xu yanbin, Wang da
School of Electrical Engineering and
Automation
Tianjin University, Tianjin, China
huaxiangwang@tju.edu.cn

Abstract:- Image reconstruction in Electrical Resistance Tomography (ERT) is an ill-posed nonlinear inverse problem. Considering the influence of the sparse measurement data on the quality of the reconstructed image, the l_1 regularized least-squares program (l_1 regularized LSP), which can be cast as a second order cone programming problem, is introduced to solve the inverse problem in this paper. A normally used method of implementing the l_1 regularized LSP is based on the interior point method whose main drawback is the relatively slow convergence speed. To meet the need of high speed in ERT, the fast iterative shrinkage-thresholding algorithm (FISTA) is employed for image reconstruction in our work. Simulation results of the FISTA and l_1 regularization algorithm show that the l_1 regularized LSP is superior to the l_2 regularization method, especially in avoiding the over-smoothing of the reconstructed image. In addition, to improve the convergence speed and imaging quality in FISTA algorithm, the initial guess is calculated with the conjugate gradient method. Comparative simulation results demonstrate the feasibility of FISTA in ERT system and its advantage over the l_1 regularization method.

Key-Words:- electrical resistance tomography; l_1 regularization method; interior-point method; iterative shrinkage-thresholding algorithm; linear inverse problem

1 Introduction

Electrical tomography (ET) has been investigated extensively during the past decades as a visualization and measurement technique [1]. It has advantages of low cost, rapid response, portability, non-invasive, safety and so on. Electrical tomography is based on the use of an array of sensing elements located around the circumference of a pipe or vessel [2]. For electrical resistance tomography (ERT), different excitation schemes or current patterns can be applied to the electrodes and the resulting changes in voltage are measured [3]. Based on the current-voltage relationship, the electrical properties of the internal distribution can be reconstructed. The major challenges with ERT are the relatively low image resolution, nonlinearity and ill-posedness [4] [5].

Conventional image reconstruction methods, such as conjugate gradient method, Landeweber method [6], Tikhonov regularization method [7] [8] [9] and so on, are

optimization methods based on 2-norm. The methods based on 2-norm which are useful to deal with those smoothness signals are not effectively for the sparse signal. The signal of ERT reconstruction image is sparse and ill-posed, so the reconstructed images based on 2-norm method have fuzzy boundaries and the images quality are not perfect. In this paper, the least square method based on 1-norm (l_1 -regularized least-squares program, l_1 -regularized LSP) [10] [11] [12] for ERT image reconstruction is presented. The problem can be cast as a second order cone programming problem and thus could be solved by l_1 algorithm via interior methods [11] [13]. However, in most applications, the matrix is large scale and the method is shown to converge very slowly. To improve the compute speed, we adopt the fast iterative shrinkage-thresholding algorithm (FISTA) [14]. In the optimization literature, this algorithm can be traced back to the proximal forward-backward iterative scheme introduced in [15] [16] within the general

framework of splitting methods. Another interesting recent contribution including very general convergence results by proximal forward-backward algorithms under various conditions and settings relevant to linear inverse problems can be found in [17]. The experimental results show that the FISTA algorithm can improve not only the computing speed but also the quality of reconstruction images .

In section 2, we introduce the ERT principle and the mathematics model, the solution of forward problem and the inverse problem. Section 3, those regularized methods for the inverse problems based on 2-norm and 1-norm are introduced. In section 4, we present l_1 -regularized least-squares program, including the ll_ls algorithm via interior methods and the FISTA algorithm. In section 5, we provide the numerical simulation results for ERT inverse problems which indicate that the FISTA algorithm can be faster and more effective than the ll_ls algorithm. In particular, when we adopt the 50th iteration result of conjugate gradient instead of vector 0 as the initial value, the speed of ISTA is faster and the reconstruction images are approximate to the true images. Section 6 closes the paper with a summary of our findings.

We provide here a brief summary of the notations used throughout the paper. Matrices are bold capital, vectors are bold lowercase and scalars or entries are not bold. For instance, \mathbf{X} is a matrix and X_{ij} is its (i,j) th entry. Likewise, \mathbf{x} is a vector and x_i is its i th component. The adjoint of a matrix \mathbf{X} is \mathbf{X}^* and similar for vectors. $\|\mathbf{x}\|$ denotes the Euclidean norm of \mathbf{x} . The spectral norm of a matrix \mathbf{A} is denoted by $\|\mathbf{A}\|_2$. The inner product of two vectors $\mathbf{x}, \mathbf{y} \in \mathbb{R}^n$ is denoted by $\langle \mathbf{x}, \mathbf{y} \rangle = \mathbf{y}^T \mathbf{x}$.

2 ERT Principle

The aim of image reconstruction for ERT is to obtain the conductivity distribution σ using the boundary voltage vector \mathbf{V} and injected current vector \mathbf{I} . According to Maxwell's electromagnetic field theory [2], the physical model of the sensitive field for ERT system

can be derived. Maxwell's equations in an inhomogeneous medium can be written as:

$$\mathbf{J} = \sigma \cdot \mathbf{E} \tag{1}$$

$$\nabla \cdot \mathbf{J} = 0 \tag{2}$$

$$\mathbf{E} = -\nabla \phi \tag{3}$$

where \mathbf{J} is the current density vector, σ the conductivity, \mathbf{E} the electric field, ϕ the potential distribution. According to the equations (1)-(3), σ satisfies

$$\nabla \cdot (\sigma \cdot \nabla \phi) = 0 \tag{4}$$

Using Ohm's law, the Neumann boundary condition of ERT can be expressed as

$$\int_{e_l} \sigma \frac{\partial \phi}{\partial \mathbf{n}} dS = I_l, \quad x \in e_l, l = 1, 2, \dots, L \tag{5}$$

$$\sigma \frac{\partial \phi}{\partial \mathbf{n}} = 0, \quad x \in \partial\Omega \setminus \bigcup_{l=1}^L e_l \tag{6}$$

where \mathbf{n} is the outward pointing normal vector to $\partial\Omega$, I_l the injection current of electrode l .

With the aid of physical modeling and FEM discretization skill, a deterministic observation model of ERT can be written as

$$\mathbf{V} = \mathbf{U}(\sigma; \mathbf{I}) = \mathbf{R}(\sigma) \mathbf{I} \tag{7}$$

where $\mathbf{U}(\sigma; \mathbf{I})$ is the forward model mapping σ and \mathbf{I} to \mathbf{V} , and $\mathbf{R}(\sigma) \mathbf{I}$ is the model mapping σ to resistance. This model depends nonlinearly on the conductivity σ and linearly on the current \mathbf{I} [5].

Based on the principle that a small change in conductivity can be reconstructed accurately by considering the linear problem, Jacobi matrix is proposed. It describes the changes in the measured voltages on the electrodes due to small changes in conductivity of the elements in a cross section, so that it can also be called sensitivity matrix in ERT. A linear approximation of an ERT model takes the following form:

$$\delta \mathbf{U} = \mathbf{U}'(\sigma_0) \delta \sigma = \mathbf{J} \delta \sigma \tag{8}$$

where $\delta \sigma$ is the change in conductivity, $\delta \mathbf{U}$ is the perturbation of boundary voltage due to the change of σ and \mathbf{J} is the Jacobi matrix at σ_0 , i.e., the partial derivatives of voltages with respect to conductivity, which is called sensitivity map in ERT.

ERT is an imaging technique which aims at estimating the interior conductivity of an unknown object. ERT system consists of sensing electrodes, data collection system, image reconstruction and visualization unit. A common ERT system is illustrated in Figure-1.

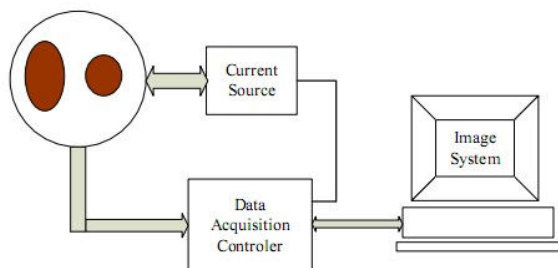


Fig. 1: Configuration of ERT System

The ERT problem consists of two parts: the forward problem and the inverse problem. The forward problem of ERT is to solve the distribution of electromagnetic field by the known distribution of object field, initial and boundary condition of sensing field. It can be commonly solved by Finite Element Method (FEM) via COMSOL Multiphase which is widely used as electromagnetic FEM simulation software. The inverse problem of ERT, namely image reconstruction aims at approximating the interior conductivity distribution by injected electrical currents and measured resulting boundary voltages. The problem is a typical ill-posed inverse problem because of the fewer measurements and the soft-field characteristics. The performance of its ill-condition is:

- 1) The singular values of J decrease and tend to zero.
- 2) The condition number of J ($\text{cond}(J)$), the ratio of the largest singular value to the smallest one of J , tends to ∞ .

Therefore, the solution to the ERT problem mainly depends on the inverse problem, namely, the degree of the accuracy and the computing speed of the image reconstruction algorithm.

For simplicity, we will be abbreviated to (8) as

$$Ax = b \quad (9)$$

where $A \in \mathbf{R}^{m \times n}$, $x \in \mathbf{R}^n$, $b \in \mathbf{R}^m$, $m < n$.

3 Regularized methods

A classical approach to problem (9) is the least squares (LS) approach in which the estimator is chosen to minimize the data error:

$$(\text{LS}): \quad \hat{x} = \arg \min_x \|Ax - b\|_2^2 \quad (10)$$

Generally, conjugate gradient method and Landweber method are originally developed for solving the well-posed LS problems [19]. In ERT system, Jacobian matrix A is underdetermined, namely $m < n$. Since the singular values of matrix A gradually decay to zero, the linear image reconstruction is ill-condition and the LS solution is unstable. To overcome this difficulty, regularized methods are required to stabilize the solution.

3.1 Tikhonov algorithm

To overcome the high sparsity and ill condition of the sensitivity matrix A of ERT system, usual standard-form Tikhonov regularization scheme for the linear ill-posed problem $Ax = b$ is

$$x = \arg \min \left\{ \|Ax - b\|_2^2 + \lambda \|x\|_2^2 \right\} \quad (11)$$

where we denote $\|Ax - b\|_2^2$ the model fit and $\|x\|_2^2$ the penalty term [9]. λ is regularization parameter, which can be chosen by L-curve criterion [18], generalized cross-validation, or the quasi-optimality criterion.

The solution to the Tikhonov regularization problem can be computed by direct method, which requires $O(n^3)$ flops, when no structure is exploited. The solution can also be computed by applying iterative (indirectly) method (e.g., the conjugate gradients method) to the linear system of equations $(A^T A + \lambda I)x = A^T b$. Iterative methods are efficient especially when there are fast algorithms for the matrix vector multiplications with the data matrix A and its transpose A^T , which is the case when the matrix is sparse or has a special form such as partial Fourier and wavelet matrices.

Both conjugate gradient and Tikhonov regularization methods are based on 2-norm. The solutions are continuous or piecewise continuous, so the reconstruction images are unavoidable smoothed and have blurry edges. It needs other image processing to obtain ideal effect.

3.2 l_1 -Regularized LSP

With the development of compressive sensing theory, another regularization method that has attracted a revived interest and considerable amount of attention in the signal processing literature is l_1 -regularization in which one seeks to find the solution of

$$\mathbf{x} = \arg \min \left\{ \|\mathbf{Ax} - \mathbf{b}\|_2^2 + \lambda \|\mathbf{x}\|_1 \right\} \quad (12)$$

where $\|\mathbf{x}\|_1$ stands for the sum of the absolute values of the components of \mathbf{x} . We call (12) an l_1 -regularized least squares program (l_1 -regularized LSP), see [10] [12] [13]. l_1 -regularized LSP yields a sparse vector \mathbf{x} which has relatively a few nonzero coefficients. The underlying idea in dealing with the l_1 norm regularization criterion is that most images have a sparse representation in the wavelet domain. The presence of the l_1 term is used to induce sparsity in the optimal solution of (9). Another important advantage of the l_1 regularization over the l_2 regularization is that as opposed to the latter, l_1 regularization is less sensitive to outputs, which in image processing applications correspond to sharp edges.

We list some basic properties of l_1 -regularized LSP, pointing out the similarities and the difference with l_2 -regularized LSP [10]:

- (a) Nonlinearity. Tikhonov regularization yields a vector \mathbf{x} which is a linear function of the observation \mathbf{b} . By contrast, l_1 -regularized LSP yields a vector \mathbf{x} , which is not linear in \mathbf{b} .
- (b) Finite convergence to zero as $\lambda \rightarrow \infty$. As in Tikhonov regularization method, the optimal solution tends to zero as $\lambda \rightarrow \infty$. For l_1 -regularized LSP,

however, the convergence occurs for a finite value of λ :

$$\lambda \geq \lambda_{\max} = \left\| 2\mathbf{A}^T \mathbf{b} \right\|_{\infty}.$$

For $\lambda \geq \lambda_{\max}$, the optimal solution of l_1 -regularized LSP is 0. In contrast, the solution of Tikhonov regularization tends to 0 only in the terms of $\lambda \rightarrow \infty$.

(c) Regularization path. The solution to Tikhonov regularization problem varies smoothly as the regularization parameter λ varies over $[0, \infty)$. By contrast, the regularization path of l_1 -regularized LSP is a piecewise linear curve on \mathbb{R}^n :

$$\mathbf{x}^{(i)} = \frac{\lambda_i - \lambda}{\lambda_i - \lambda_{i+1}} \mathbf{x}^{(i+1)} + \frac{\lambda - \lambda_{i+1}}{\lambda_i - \lambda_{i+1}} \mathbf{x}^{(i)},$$

$$\lambda_{i+1} \leq \lambda \leq \lambda_i, \quad i = 1, 2, \dots, k-1$$

Where $\mathbf{x}^{(i)}$ is the solution of the l_1 -regularized LSP

with $\lambda = \lambda_i$.

4 Algorithm Analysis

The objective function in the l_1 -regularization problem (12) is convex but not differential, so solving it is more of a computational challenge than solving l_2 -regularization problem (11). In this section, we will introduce two ways to the problem (12), l_1 -ls algorithm via interior point method and iterative shrinkage-thresholding algorithm (ISTA).

4.1 l_1 -ls Algorithm

The l_1 -ls algorithm is proposed by the compressive sensing research group from California Institute of Technology [12] [13]. The main idea is to transform (12) to a convex quadratic problem with linear inequality constraints. The equivalent quadratic program can be solved by standard convex optimization methods such as interior point methods. Standard methods can not handle large scale problems in which there are fast algorithms for the matrix vector operations with \mathbf{A} and \mathbf{A}^T . Specialized interior point methods that exploit such algorithms can prompt to large problems, as demonstrated in [10].

The whole process is to transform the l_1 -norm into a convex quadratic problem with linear inequality constraints:

$$\begin{aligned} \min \quad & \|Ax - y\|_2^2 + \lambda \sum_{i=1}^n u_i \\ \text{s.t.} \quad & -u_i \leq x_i \leq u_i, i = 1, 2, \dots, n \end{aligned} \quad (13)$$

We start by defining the logarithmic barrier for the bound constrains $-u_i \leq x_i \leq u_i$ in (13):

$$\Phi(x, u) = -\sum_{i=1}^n \log(u_i + x_i) - \sum_{i=1}^n \log(u_i - x_i)$$

The central path consists of the unique minimize value of the convex function:

$$\phi_t(x) = t \|Ax - b\|_2^2 + T - \sum_{i=1}^n \lambda x_i + \Phi(x, u)$$

as the parameter t varies from $0 \sim \infty$. Then use Newton's method as the basic principles of each iteration to minimize ϕ_t , i.e., the search direction is computed as the exact solution to the Newton system

$$H \begin{bmatrix} \Delta x \\ \Delta u \end{bmatrix} = -g$$

Where $H = \nabla^2 \phi_t(x, u) \in \mathbb{R}^{2n \times 2n}$ is the Hessian

matrix, and $g = \nabla \phi_t(x, u) \in \mathbb{R}^{2n}$ is the gradient at the current iterative (x, u) .

In this algorithm, the choice of the parameter λ is the key problem which decides the speed of the algorithm and the quality of the reconstruction images. λ changes in a range of $(0, \|2A^T b\|_\infty)$. When $\lambda \rightarrow 0$, it will approximate to the solution of the problem. When $\lambda > \|2A^T b\|_\infty$, x tends to 0. If λ is too small, it will inevitably lead to long computing time, so that the real-time property is very poor. If λ is too large, it will seriously affect the accuracy of the results. λ depends on the sparsity of the reconstruction images which can be indicated by $\|A^T b\|_\infty$. In this paper, we choose $\lambda = 0.01 \times \|2A^T b\|_\infty$ commonly.

For this algorithm, each iteration requires one multiplication by A and A^T which costs plenty of computing time.

4.2 FISTA Algorithm

In most applications, e.g., an image deblurring, the problem is not only large scale but also involves dense matrix data, which often precludes the use and potential advantage of sophisticated interior point method. Moreover, some experiences indicate that ll_ls algorithm costs more computing time and has poor real-time [21], so the algorithm does not satisfy the requirement to the real time of the ERT system.

In the recent study [22], problem (12) is reformulated as a box-constrained quadratic problem and solved by a gradient projection algorithm. One of the most popular methods for solving (12) is in the class of iterative shrinkage-thresholding algorithm (ISTA), where each iteration involves matrix-vector multiplication involving A and A^T followed by a shrinkage/soft-threshold step [23] [24]. Specifically, the general step of ISTA is

$$x_{k+1} = T_{\lambda t} (x_k - 2tA^T(Ax_k - b)) \quad (14)$$

Where t is an appropriate step-size and $T_\alpha : \mathbb{R}^n \rightarrow \mathbb{R}^n$ is the shrinkage operator defined by

$$(T_\alpha)_i = (|x_i| - \alpha)_+ \text{sgn}(x_i) \quad (15)$$

Consider the unconstrained minimization problem of a continuously differentiable function $f : \mathbb{R}^n \rightarrow \mathbb{R}^n$:

$$(U) \quad \min \{f(x) : x \in \mathbb{R}^n\}$$

One of the simplest methods for solving (U) is the gradient algorithm which generates a sequence $\{x_k\}$ via:

$$x_0 \in \mathbb{R}^n, \quad x_k = x_{k-1} - t_k \nabla f(x_{k-1}) \quad (16)$$

Where $t_k > 0$ is a suitable step-size. It is very well

known that the gradient iteration (16) can be viewed as a proximal regularization of the linearized function f

at x_{k-1} , and written equivalently as

$$x_k = \arg \min_x \left\{ f(x_{k-1}) + \langle x - x_{k-1}, \nabla f(x_{k-1}) \rangle + \frac{1}{2t_k} \|x - x_{k-1}\|^2 \right\}$$

$$x_k = P_L(x_{k-1})$$

Adopting this basic gradient idea to the nonsmooth l_1 regularized problem

$$\min \{ f(x) + \lambda \|x\|_1 : x \in \mathbb{R}^n \} \quad (17)$$

Leads to the iterative scheme

$$x_k = \arg \min_x \left\{ f(x_{k-1}) + \langle x - x_{k-1}, \nabla f(x_{k-1}) \rangle + \frac{1}{2t_k} \|x - x_{k-1}\|^2 + \lambda \|x\|_1 \right\}$$

After ignoring constant terms, this can be written as

$$x_k = \arg \min_x \left\{ \frac{1}{2t_k} \|x - (x_{k-1} - t_k \nabla f(x_{k-1}))\|^2 + \lambda \|x\|_1 \right\}$$

which is a special case of the scheme for solving (17). Since the l_1 norm is separable, the computation of x_k reduced to solve a one dimensional minimization problem for each of its components, which by simple calculus produces

$$x_k = T_{\lambda t_k}(x_{k-1} - t_k \nabla f(x_{k-1})),$$

where $T_\alpha : \mathbb{R}^n \rightarrow \mathbb{R}^n$ is the shrinkage operator given in

(15). Thus, with $f(x) = \|Ax - b\|^2$, the popular ISTA is recovered (14).

The key of ISTA is the choice of step-size t . [14] discussed the convergence of the algorithm and the choice criteria of the parameter t . Let $f(x) = \|Ax - b\|^2$,

$g(x) = \lambda \|x\|_1$ ($\lambda > 0$). $\nabla f = 2A^T(Ax - b)$ is the gradient

of f and $L := L(f) = 2\lambda_{\max}(A^T A)$ is the Lipschitz

constant of ∇f . Then (12) reduces to the basic shrinkage method (14) with $t = 1/L(f)$. Define

operator $P_L : \mathbb{R}^n \rightarrow \mathbb{R}^n$, $P_L(x) = T_{\lambda t}(x_k - 2tA^T(Ax_k - b))$,

$t = 1/L(f)$. The process of ISTA algorithm with constant step-size is as follows:

Input: $L = 2\lambda_{\max}(A^T A)$
 Step 0: take initial value $x_0 \in \mathbb{R}^n$
 Step $k(k \geq 1)$: computer

ISTA is a natural extension of the gradient method. Therefore, ISTA belongs to the class of first order methods, that is, optimization methods that are based on function values and gradient evaluation. It is well known that for large-scale problems first order methods are often the only practical option, but as alluded to above it has been observed that the sequence $\{x_k\}$ converges quite slowly to a solution. In fact, as a first result we further confirm this property by proving that ISTA behave like

$$F(x_k) - F(x^*) \approx O(1/k)$$

namely, shares a sublinear global rate of convergence.

To improve the complexity result, a fast iterative shrinkage-thresholding algorithm (FISTA) is introduced [14]. FISTA keeps the simplicity of ISTA but shares the improved rate $O(1/k^2)$ of the optimal gradient method for minimizing smooth convex problems. The process of FISTA algorithm with constant step-size is as follows:

Input: $L = 2\lambda_{\max}(A^T A)$
 Step 0: take initial value $y_1 = x_0 \in \mathbb{R}^n, t_1 = 1$
 Step $k(k \geq 1)$: computer

$$x_k = P_L(y_k),$$

$$t_{k+1} = \frac{1 + \sqrt{1 + 4t_k^2}}{2},$$

$$y_{k+1} = x_k + \left(\frac{t_k - 1}{t_{k+1}} \right) (x_k - x_{k-1}).$$

The main difference between FISTA and ISTA is that the iterative shrinkage operator P_L is not employed on the previous point x_{k-1} , but rather at the point y_k which uses a very specific linear combination of the previous two points $\{x_{k-1}, x_{k-2}\}$. Obviously the main computational effort in both ISTA and FISTA remains the same, namely, in the operator P_L .

5 Simulation Experiment Results

In this section we show the performance of the FISTA, Landweber, l_1 -ls and Tikhonov regularization method. Adjacent excitation and measurement is adopted for a 16 electrodes ERT system. Reconstruction based on MATLAB7.6 is carried out using a PC with a CPU of Pentium(R) 4 2.93GHz and 1GB RAM.

Simulations were carried out to evaluate the performance of these four different ways. The forward problem was solved using a complete electrode model and a finite element method (FEM) by COMSOL Multiphysics. A mesh of adaptive first-order triangular elements, produced in COMSOL, was used for the forward calculations (see Figure 2(a)). The conventional adjacent current injection and voltage measurement strategy were used. The reconstructed image presents conductivity values using another mesh with 812 square elements (see figure 2(b)).

(a) Mesh used for forward problem (b) Mesh used for inverse problem

Fig. 2: Meshes for forward and inverse problems.

Three conductivity distributions, as shown in figure 3-5, were simulated. The contrast of background and objects conductivity was 1:2. $\pm 1\%$ Gaussian random noise, corresponding to the typical noise levels in real measurement systems, was added to the simulated voltages. Images were reconstructed by the Landweber algorithm (Landweber), the Tikhonov regularization method (Tikhonov), l_1 -ls algorithm (l_1 -ls) and FISTA algorithm (FISTA). Fig. 3 shows the reconstruction results using these four algorithms. Table 1 and Table 2 show the iterative times and the copution time of each algorithm.

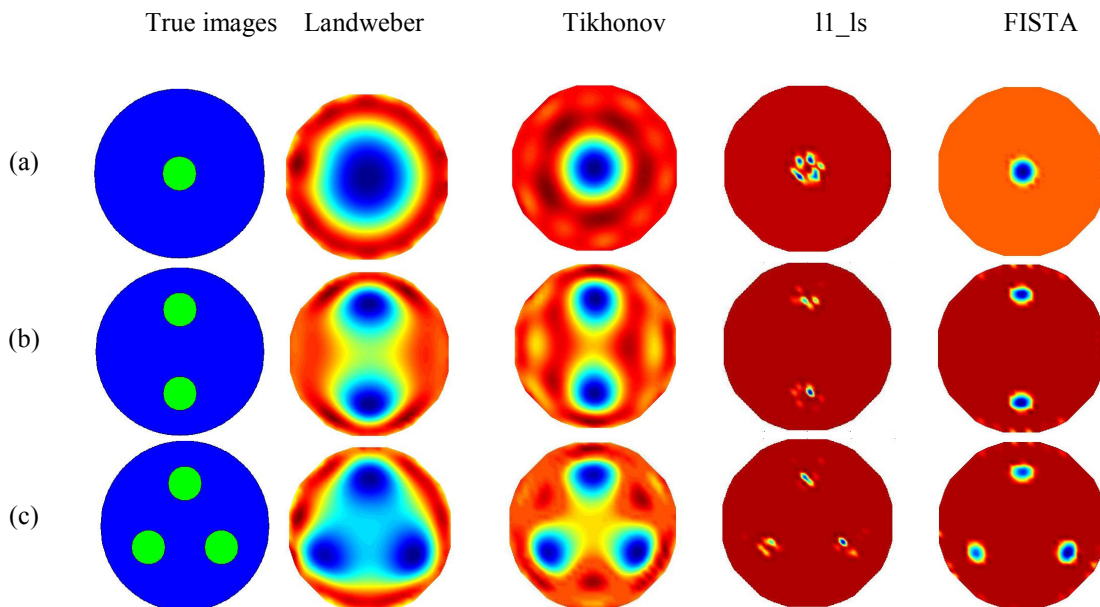
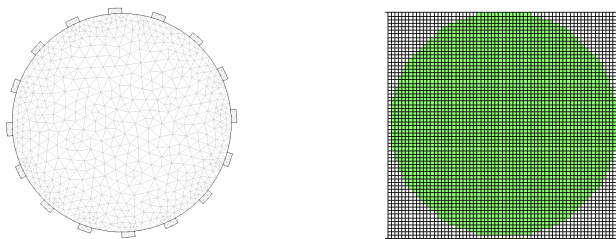


Fig. 3: Reconstructed images of simulated data with conductivity contrast of 1:2, using Landweber algorithm, Tikhonov regularization method, l_1 -ls algorithm and FISTA algorithm. The medium ration is 0.2:1.

Table 1: Comparison of four different algorithms in terms of iterative times

Conductivity distribution	Landweber	Tikhonov	L1-ls	FISTA
(a)	300	500	1271	400
(b)	300	500	1187	400
(c)	300	500	1064	400

Table 2: Comparison of four different algorithms in terms of computation time (unit:s)

Conductivity distribution	Landweber	Tikhonov	L1-ls	FISTA
(a)	0.073420	0.113301	7.939994	0.471249
(b)	0.081700	0.1202539	7.401061	0.451912
(c)	0.075112	0.1231321	7.033425	0.447283

From the above, we can see that the artifacts of the reconstructed images in the first two columns are largely reduced and the objects are located more accurately using the l_1 -regularized LSP (including the l_1 -ls algorithm and FISTA algorithm). The reconstruction results obtained using the l_2 regularized least square programs (including the Tikhonov regularized method and Landweber algorithm) have blurry edges, which make it hard to identify the flow pattern from the reconstructed image. Comparing the l_1 -ls algorithm with the FISTA algorithm, we can easily find that the reconstruction images obtained

using the FISTA algorithm are close to the real phantoms. By contrast, the reconstructed images of the l_1 -ls algorithm can be located accurately but the image quality is relatively poor. Furthermore, from Table 2, we can see that the computation time required for reconstructing an image of the FISTA algorithm has greatly improved compared with the l_1 -ls algorithm, although the speed is much slowly by comparison with those of the l_2 regularized least square programs (Landweber algorithm and Tikhonov regularized method).

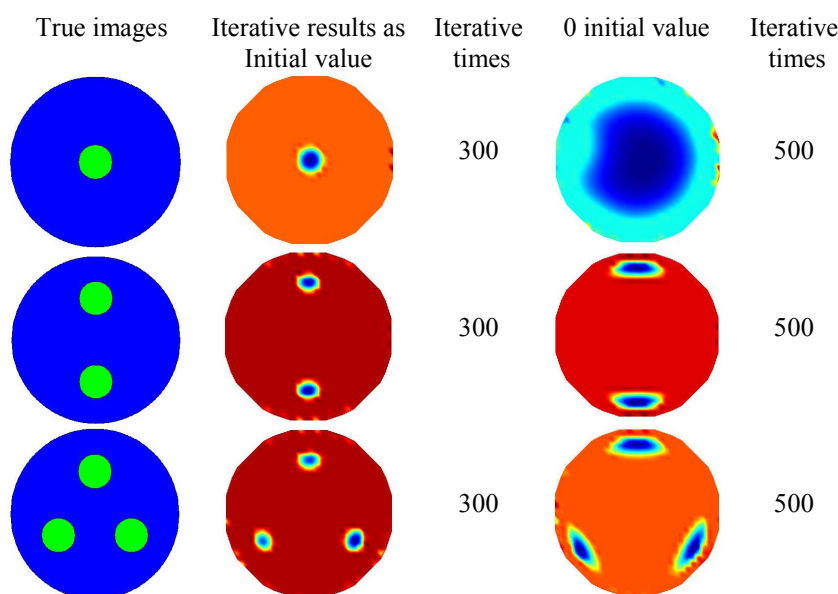


Fig. 4: Reconstruction images and the iterative times using 50th iterative results of the conjugate gradient algorithm as initial value and vector 0 as iterative

iterative scheme for solving the inverse problem in ERT system. Compared to the ℓ_1 -ls algorithm, it is both faster and more accurate. Furthermore, its potential for designing faster algorithms in other research areas and being applied in other types of regularization are the topics of our future work.

Acknowledgments

The authors would like to thank the National Natural Science Foundation of China (60820106002, 50937005) and the Natural Science Foundation of Tianjin Municipal Science and Technology Commission (11JCYBJC06900) for supporting this work. This work was also supported by Seed Foundation of Tianjin University.

References:

- [1] N. Reinecke, D. Mewes, Recent development and industrial/research applications of capacitance tomography, *Measurement Science and Technology*, vol. 7, No. 3, 1996, pp. 223-246.
- [2] T. York. Status of electrical tomography in industrial applications, *Journal of Electronic Imaging*, vol. 10, No. 3, 2001, pp. 608-619.
- [3] D. Willian, R. Abelardo. Electrical resistance tomography , *Society of Exploration Geophysicists*, vol. 23, No. 5, 2004, pp. 438-442.
- [4] F. Dong, Y. Xu, Application of electrical resistance tomography in two-phase flow measurement, *Journal of engineering thermophysics*, vol. 27, No. 5, 2006, pp. 791-794.
- [5] H. Wang, J. Wang, L. Hu, Optimal design of ERT/ECT dual—modality sensing electrode array, *Journal of Tianjin University*, vol. 8, No. 8, 2008, pp. 911—918.
- [6] O. Daniel, J. Tadeusz, D Mauricio, Accurate interpolation with high-resolution time-variant Radon transforms, *Society of Exploration Geophysicists*, vol. 67, No. 2, 2002, pp. 644-656.
- [7] Y. Li, Z. Huang, H. Ji, Study on image reconstruction algorithm of electrical resistant tomography for two-phase flow measurement, *Journal of Zhejiang University(Engineering Science)*. Vol. 37, No. 4, 2003, pp. 382-385.
- [8] H. Wang, Y. He, X. Zhu, Regularization parameter optimum of electrical capacitance tomography based on L-curve method, *Journal of Tianjin University*, vol. 39, No. 3, 2006, pp. 306-309.
- [9] J. Li, *Regularization methods and application of ill-posed problems*. Beijing: Science Publishing Company ,2005.
- [10] S. Kim, K. Koh, M. Ltig et al, An Interior-Point Method for Large-Scale ℓ_1 -Regularized Least Squares, *IEEE Journal of Selected Topics in Signal Processing*, vol. 1, No. 4, 2007, pp. 606-617.
- [11] E. Candès, J. Romberg, T Tao, Stable signal recovery from incomplete and in accurate measurements, *Communications on Pure Applied Mathematics*, vol. 59, No. 8, 2005, pp. 1207-1223.
- [12] D. Donoho, For most large underdetermined systems of linear equations, the minimal ℓ_1 norm near-solution approximates the sparsest near-solution, *Communications on Pure and Applied Mathematics*, vol. 59, No. 7, 2006, pp. 907-934.
- [13] D. Donoho, Compressed Sensing, *IEEE Trans. Info. Theory*, vol. 52, No. 4, 2006, pp. 1289-1306.
- [14] A. Beck, M. Teboulle, A fast iterative shrinkage-thresholding algorithm for linear inverse problems, *SIAM Journal of imaging sciences*, vol.2, No.1, 2009, pp. 183-202.
- [15] R. J. Bruck, On the weak convergence of an ergodic iteration for the solution of variational inequalities for monotone operators in Hilbert space, *Journal of Mathematical Analysis and Applications*, vol. 61, No. 1, 1977, pp. 159-164.
- [16] G. B. Passty, Ergodic convergence to a zero of sum of monotone operators in Hilbert space, *Journal of Mathematical Analysis and Applications*, vol.72, No. 2, 1979, pp. 383-390.
- [17] P. L. Combettes, V R Waunders, Signal recovery by proximal forward-backward splitting, *Multiscale Modeling and Simulation*, vol. 4, No. 4, pp. 1168-1200, 2005.
- [18] P. C. Hansen, Analysis of discrete ill-posed problems by means of the L curve, *SIAM Review*, vol. 34, No. 4, 1992, pp. 561-580.
- [19] Y. Yuan, W. Sun, *Optimization Theory and method*, Beijing: Science Publishing Company ,2007.

- [20] A. B. Tal, A. Nemirovski, Lectures on modern convex optimization: analysis, algorithms and engineering applications, *MPS/SIAM Ser. Optim.*, SIAM, Philadelphia, 2001.
- [21] J. Lei S. Liu, Z. Li, Image reconstruction iteration algorithm based on 1-norm for electrical capacitance tomography, *Chinese Journal of Scientific Instrument*, vol. 29, No.7, 2008, pp. 1355-1358.
- [22] M. A. T Figueiredo, R. D. Nowark, S. J. Wright, Gradient projection for sparse reconstruction: Application to compressed sensing and other inverse problem, *IEEE Journal Selected Topics in Signal processing*, vol. 1, No. 4, 2007, pp. 586-597.
- [23] K. Bredies, D. Lorenz. Iterative soft-thresholding converges linearly, Technical report, 2008, available on line at <http://arxiv.org/abs/0709.1598v3>.
- [24] C. Vonesch, M. Unser, A Fast iterative thresholding algorithm for wavelet-regularized deconvolution, *In processing of the SPIE optics and photonics on mathematical methods:wavelet VII*, vol. 6701, San Diego, CA, 2007, pp. 785-800.